Author Manuscript Published OnlineFirst on September 6, 2017; DOI: 10.1158/1535-7163.MCT-17-0233
Author manuscripts have been peer reviewed and accepted for publication but have not yet been edited.

The p97 inhibitor CB-5083 is a unique disrupter of protein homeostasis in models of Multiple Myeloma.

Ronan Le Moigne*[1], Blake T. Aftab*[2], Stevan Djakovic[1], Eugen Dhimolea[3], Eduardo Valle[1], Megan Murnane[2], Emily M. King[3], Ferdie Soriano[1], Mary-Kamala Menon[1], Zhi Yong Wu[1], Stephen T. Wong[1], Grace J. Lee[1], Bing Yao[1], Arun P. Wiita[4], Christine Lam[4], Julie Rice[1], Jinhai Wang[1], Marta Chesi[5], P. Leif Bergsagel[5], Marianne Kraus[6], Christoph Driessen[6], Szerenke Kiss von Soly[1], F. Michael Yakes[1], David Wustrow[1], Laura Shawver[1], Han-Jie Zhou[1], Thomas G. Martin III[2], Jeffrey L. Wolf[2], Constantine S. Mitsiades[3], Daniel J. Anderson[1], Mark Rolfe[1].

*Contributed equally to this work

Affiliations

[1]Cleave Biosciences, Inc., Burlingame CA 94010 USA.

[2]Department of Medicine, Division of Hematology & Oncology, University of California San Francisco, San Francisco, CA 94158 USA.

[3]Department of Medical Oncology, Dana-Farber Cancer Institute, Harvard Medical School, Boston, Massachusetts, USA.

[4]Department of Laboratory Medicine, University of California, San Francisco, San Francisco, CA 94107 USA

[5]Comprehensive Cancer Center, Mayo Clinic, 13400 E Shea Blvd, Scottsdale, AZ, 85259, USA

[6]Experimental Oncology and Hematology, Department of Oncology and Hematology, Kantonsspital St. Gallen, 9007, St. Gallen, Switzerland

Address correspondence to:

Ronan Le Moigne,

866 Malcolm Rd, #100

Burlingame. CA, 94010

Phone : 650-443-3000

E-mail: ronan.lemoigne29@gmail.com

Abstract

Inhibition of the AAA ATPase, p97, was recently shown to be a novel method for targeting the ubiquitin proteasome system (UPS) and CB-5083, a first in class inhibitor of p97, has demonstrated broad antitumor activity in a range of both hematological and solid tumor models. Here, we show that CB-5083 has robust activity against multiple myeloma (MM) cell lines and a number of *in vivo* MM models. Treatment with CB-5083 is associated with accumulation of ubiquitinated proteins, induction of the unfolded protein response (UPR) and apoptosis. CB-5083 decreases viability in MM cell lines and patient derived MM cells, including those with background proteasome inhibitor (PI) resistance. CB-5083 has a unique mechanism of action that combines well with PIs which is likely owing to the p97-dependent retro-translocation of the transcription factor, Nrf1, which transcribes proteasome subunit genes following exposure to a PI. *In vivo* studies using clinically relevant MM models demonstrate that single-agent CB-5083 inhibits tumor growth and combines well with MM standard of care agents. Our preclinical data demonstrate the efficacy of CB-5083 in several MM disease models and provide the rationale for clinical evaluation as monotherapy and in combination in MM.

Introduction

Inhibition of the β5 peptidase of the 20S proteasome with bortezomib provided clinical validation for targeting protein homeostasis and transformed the standard of care in both multiple myeloma and mantle cell lymphoma (1,2). The recent clinical successes of the second generation PIs, carfilzomib and ixazomib, have built upon this therapeutic strategy and confirmed the clinical susceptibility of multiple myeloma to inhibitors of the ubiquitin proteasome system (UPS) (3). The dependency of multiple myeloma on protein homeostasis pathways is owing to the fact that they retain the characteristic biology of normal plasma cells, namely synthesis and secretion of large amounts of immunoglobulins (4). However, multiple myeloma remains an incurable disease, even with the introduction of new therapeutic modalities over the last two years and hence there is a need to develop new agents intervening in the myeloma cell's protein homeostasis pathways at different points compared to PIs.

Recently, inhibition of p97, has emerged as a new approach for targeting protein homeostasis in tumor cells (5,6). Also known as valosin-containing protein, p97 is an essential and conserved member of the AAA family of adenosine triphosphatases (AAA ATPases) and is a key regulator of protein homeostasis. p97 generates mechanical force via ATP hydrolysis and this force is used to extract proteins from macromolecular complexes and organelles. p97 is involved in multiple biological processes including protein homeostasis, endoplasmic reticulum associated degradation (ERAD), autophagy, chromatin remodeling and Golgi reassembly through its interaction with cofactors (7). Reducing p97 levels with siRNA causes ER stress and activates apoptosis through the unfolded protein response (UPR), a pathway that acts both to resolve

unfolded protein stress and to trigger cell death when the buildup of such unfolded proteins becomes irresolvable (5,8,9).

CB-5083 is a potent and highly selective inhibitor of the D2 ATPase domain of p97 (10,11). Inhibition of p97 by CB-5083 activates the UPR and subsequently induces apoptosis in a wide variety of hematological and solid tumor cell lines. CB-5083 was shown to be the first inhibitor of p97 to demonstrate significant tumor growth inhibition in vivo and was also active in solid tumor models where PIs were inactive (10). Since CB-5083 disrupts protein homeostasis upstream of the proteasome, we wanted to assess whether targeting p97 would have different effects from PIs in various in vitro and in vivo models of MM. Our studies described here suggest there is a therapeutic rationale for targeting p97 in MM and that inhibition of p97 is biologically distinct from targeting the proteasome.

Materials and methods

Cell culture and reagents

Bortezomib and carfilzomib resistant AMO-1 cell lines were generated as described previously (12,13). Cancer cell lines were obtained from American Type Culture Collection (ATCC) or Deutsche Sammlung von Mikroorganismen und Zellkulturen GmbH (DSMZ) between 2011 and 2015 and were cultured according to supplier's instructions. Fresh bone marrow samples from adult patients with MM were extracted at the respective hospital centers during the patient's regular treatment schemes, following clinical practice at the center. These samples were treated with CB-5083, bortezomib or carfilzomib ex vivo and viability of the CD38/CB138 negative and positive populations were analyzed with the ExviTech platform (14). Lenalidomide, bortezomib, carlfizomib and ixazomib were obtained from Selleck Chemicals. Thapsigargin and dexamethasone were obtained from Sigma.

Immunofluorescence

Cells were cultured in clear bottomed, tissue culture-treated 384-well plates and treated with compound in well duplicates. For immunofluorescence staining, paraformaldehyde (4% final) was added to plates after 8 hr of treatment. Cells were blocked in PBS with 1% BSA, 0.3% Triton-X100 and Hoechst (1:10,000) for 1 hour and then incubated in primary antibodies at 4 degrees Celsius for 16 hr. Cells were washed three times in PBS and secondary antibodies were added for 2 hours at 25 degrees Celsius. Cells were washed four times in PBS and imaged with an automated wide field fluorescence microscope (Cell Insight, Thermo Fisher Scientific).

Automated image analysis was written in Matlab (Mathworks) to count nuclei, mask cellular compartments and measure fluorescence intensities within cellular compartments.

Western blotting

Cells or ex vivo lysates were lysed with RIPA buffer supplemented with protease inhibitors (Roche Applied Science) and phosphatase inhibitors (Sigma). Lysates were cleared and protein was quantified by Pierce BCA protein assay kit. Western blotting was performed using the Novex® NuPAGE® SDS-PAGE Gel system. Briefly, 10 µg of protein was resolved on 4-12% Bis-Tris gradient gels and then transferred onto Nitrocellulose membranes. Membranes were blocked for one hour at room temperature in TBS + 0.1% Tween (TBST) with 5% non-fat dry milk. Membranes were probed overnight at 4 degrees Celsius with primary antibodies (Supplementary Table S1). Membranes were washed three times in TBST and then incubated with goat anti-rabbit or goat anti-mouse secondary antibodies (Supplementary Table S1) for 1 hour at room temperature. Membranes were then washed three times with TBST and developed with SuperSignal West Dura Chemiluminescent Substrate. Images were taken using a BioRad Gel Doc Imager system, exported as TIF files and cropped using NIH ImageJ.

Cell viability assays

Viability assays conducted in myeloma cell lines, stably transduced with firefly luciferase, were carried out as previously described (15,16). For co-culture assays, short-term ex vivo cultures of $CD138^-$ fractions from bone marrow aspirates were cultured for 3 passages. HS5, HS27A, or patient derived cultures were seeded into assay plates 16 hours (hr) prior to additional of MM

cells. Cocultures were grown for 24hr, then after drug addition, MM cell viability was monitored using luciferase as described above. GI_{50} values were derived from dose-response curves plotted and fitted using Prism (GraphPad). Cell titer glo assays were conducted as previously described(10).

Gene expression analysis

Mean gene expression values were calculated for all solid tumor derived cell lines versus MM cell lines using the CCLE (https://portals.broadinstitute.org/ccle/home) gene expression data. Difference in gene expression between the two cell groups was calculated using a student's t-test. Genes overexpressed in MM with a p-value >0.001 were analyzed using ENRICHR (http://amp.pharm.mssm.edu/Enrichr/).

Transcriptome analysis

MM cells were treated with CB-5083, bortezomib, or with DMSO as a control. RNA samples were converted into cDNA libraries using the Illumina TruSeq Stranded mRNA sample preparation kit (Illumina # RS-122-2103). The pipeline mRNAv8-RSEM (EA-Quintiles) was used to analyze RNA-seq data. Total RNA extraction, purification and data analysis were performed as previously described (10). The RNA sequencing data has been deposited in NCBI's Gene Expression Omnibus (17) and is accessible through GEO Series accession number GSE101923 (https://www.ncbi.nlm.nih.gov/geo/query/acc.cgi?acc= GSE101923). For gene ontology analysis, samples were processed as previously described (10).

In vivo models

All experiments involving animals were approved by an institutional Animal Care and Use Committee. Female athymic nude mice and SCID Beige mice, 5-8 weeks of age and weighing approximately 20-25 grams were purchased from Envigo (Cambridgeshire, UK). Cancer cell line xenografts were established by implanting 1 X 10^6 - 20 X 10^6 cells subcutaneously or intravenously. For the ortho-metastatic models, bi-weekly luciferase imaging was conducted using the Xenogen IVIS Spectrum Imaging System and Living Image software. Overall tumor burden was both quantified in photons/sec and visualized by heatmap representations of radiance (photons/sec/cm2/sr). CB-5083, lenalidomide, ixazomib and the CB-5083 vehicle (0.5% methyl cellulose in water) were administered by oral gavage, bortezomib and carfilzomib were dosed by tail vein injection and dexamethasone was administered intraperitoneally. Tumor volume and body weights were measured twice weekly and daily, respectively, throughout the study. Vk*MYC mice work and SPEP analysis was performed as described previously (18).

In vivo protein analysis

Tumors were excised, flash frozen and stored at -60°C to -90°C. Following thawing, tissues were processed as previously described(10).. Determination of cleaved PARP and CHOP accumulation in tumor lysates was performed using commercially available MesoScale kits (MSD; Rockville, MD). Determination of K48-polyubiquitin accumulation in tumor lysates was performed by developing a MesoScale assay with a K48-Ubiquitin antibody (Millipore). Total protein concentrations were determined with a BCA assay (BCA Protein Assay #23225, ThermoFisher Scientific, Rockford, IL) and then normalized to 2 mg/mL. Aliquots were added to the ELISA/MSD plate and the remaining assay procedures carried out according to the

manufacturer's protocol. Determination of circulating lambda light chain in mouse plasma was performed using a commercially available kit (Biovendor, Czech Republic).

Statistical analysis

For in vivo studies, Statistical analysis was performed using two-way analysis of variance (ANOVA) on delta tumor values in Prism (GraphPad).

Results

CB-5083 treatment leads to potent and rapid death of MM cell lines compared to solid tumor cell lines

In order to characterize the potency of cell death following exposure to CB-5083, eighteen human MM cell lines were treated with CB-5083. Following 72-hr exposure, CB-5083 showed GI_{50}s ranging from 96 to 1,152 nM, with a median GI_{50} of 326 nM (Fig. 1A). CB-5083 was less potent in immortalized or primary patient-derived bone marrow stromal cultures compared to MM cell lines (Fig. 1A, Fig. 6D). CB-5083 has potent antitumor activity in several solid tumor cell lines (10), however MM cell lines showed significantly greater overall sensitivity to CB-5083 than solid tumor cell lines (Fig. 1B).In an attempt to understand the difference in sensitivity of solid tumor versus MM cell lines, we analyzed publicly available genomic data (CCLE) via ENRICHR (http://amp.pharm.mssm.edu/Enrichr/). GO Biological Process showed the myeloma cells to have significant enrichment of ER/UPR related pathways compared to the solid tumor cells (Fig. 1C). Frequently, the levels of a drug target can influence sensitivity to its inhibitor. Therefore, we analyzed p97 protein levels in a subset of three MM and three solid tumor cell lines (Supplementary Fig. S1A) and found no correlation between p97 levels and CB-5083 sensitivity. We next analyzed the kinetics of cell death in this subset of cell lines. The MM cell lines MM1.S, AMO-1 and RPMI8226 died far more rapidly than the colon tumor cell lines HCT116 and DLD-1 and the pancreatic cancer cell line, CFPAC-1 (Fig. 1D). These data were consistent with the induction of apoptosis that peaked between 8-16 hr in the MM cell lines versus 36-48 hr in the colon and pancreatic tumor cell lines (Fig. 1E). This rapid kinetic of cell

death was confirmed using an independent viability assay (time-lapse bioluminescence) (Supplementary Fig. S1B and S1C). In conclusion, we found that MM cells grown in the presence of CB-5083 are highly sensitive, die rapidly and have a baseline gene expression profile that is distinct from less sensitive solid tumor cell lines.

CB-5083 treatment activates the UPR, induces irresolvable ER stress and activates apoptosis in vitro and in vivo

p97 knockdown or inhibition with small molecules has been shown to induce endoplasmic reticulum (ER) stress and activate all three arms of the UPR (5,19). CB-5083 caused a strong induction of the UPR as measured by the phosphorylation of PERK and accumulation of sXBP1 and BiP (Fig. 2A and Supplementary Fig. S2). CB-5083 treatment led to a robust induction of the transcription factor CCAAT/enhancer-binding protein homologous protein (CHOP) which was higher than the maximum response observed with bortezomib and similar to what was seen with the ER stress agent thapsigargin.

K48-linked poly-ubiquitin accumulation, a hallmark of inhibition of protein degradation (20,21), was followed as a pathway marker for p97 inhibition (Fig. 2A-B). CB-5083, like bortezomib, induced a rapid accumulation of K48 linked poly-ubiquitinated proteins in cultured cells and xenografted MM tumors. In RPMI8226 xenografts, a single dose of CB-5083 led to plasma levels of CB-5083 that ranged from 2 to 20 µM over a period of 24 hr, sufficient to maintain significant K48 poly-ubiquitin accumulation (Fig. 2B). This dose was sufficient to activate the UPR, and CHOP protein expression increased up to 2.7-fold compared to baseline levels. Consequently,

apoptosis was activated, as demonstrated by an increase in cleaved poly-ADP ribose polymerase (cPARP) levels (Fig. 2C).

The target engagement and pathway protein modulations seen in MM cell lines in vitro and in vivo in response to CB-5083 treatment were consistent with the cellular responses to p97 inhibition, with differences noted when comparing to bortezomib.

Sensitivity and transcriptional response to CB-5083 is distinct from PIs in MM

To evaluate the similarities or differences in protein homeostasis disruption via PIs versus p97 inhibition, we compared the relative sensitivity of 18 MM cell lines to bortezomib, carfilzomib, and CB-5083 by correlating GI_{50} values across the cell line panel for all pairwise comparisons of inhibitors. The correlation for relative sensitivities of the MM cell lines to bortezomib and carfilzomib was significant ($p=0.0001$), reflecting the similar mechanism of action of both drugs (Fig. 3C). However, the relative response and sensitivity across the MM lines were not significantly correlated between CB-5083 and either PI ($p=0.613$ and 0.118 respectively; Fig. 3A and 3B).

Next, we analyzed gene expression in response to either bortezomib or CB-5083 in RPMI8226, AMO-1, and MM1.S cell lines. In these experiments, cross-comparisons of ranked gene lists associated with each agent were clearly distinct (Supplementary Fig. S3A-B). While transcripts that were most strongly induced in response to CB-5083 were also induced by bortezomib (Supplementary Fig. S3A), transcripts that were most strongly induced in response to bortezomib showed a mixed profile in response to CB-5083 (Supplementary Fig. S3B). More significant differences were noted upon analysis of ranked gene identities for bortezomib-

induced transcripts which indicated that many of the heat-shock protein family members and chaperones from the Bag family typically induced by bortezomib (22) were decreased in response to CB-5083 (Fig. 3D). Using RNAseq data, gene ontology analysis was performed to identify the pathways that were altered after bortezomib or CB-5083 treatment. In both RPMI8226 (Fig. 3E) and AMO-1 (Fig. 3F) cell lines, the gene ontology analysis showed both compounds induced similar pathways, but CB-5083 responses were predominantly focused on ER stress and UPR whereas bortezomib responses were focused more on general protein stress. Altogether, these cell viability and transcriptomic results suggest that the mechanism of action of CB-5083 and the transcriptional response it produced has some unique features compared to PIs.

Combination with PIs improves potency of CB-5083 in MM cells

We next investigated if the blockade of both p97 and the proteasome could lead to enhanced cytotoxicity. RPMI8226 cells were treated with a range of CB-5083 concentrations in the presence of various dose levels of bortezomib (Fig. 4A) or carfilzomib (Fig. 4B). When PIs were combined with CB-5083, a lower GI_{50} of CB-5083 was observed, suggesting enhanced cell killing activity. These data were confirmed in three additional MM cell lines (Supplementary Fig. S4A-C). The combination of CB-5083 with PIs was then studied in vivo. After a single dose of CB-5083 combined with a single dose of bortezomib, the combination arm showed a much more dramatic effect on the induction of K48-ubiquitin and cPARP in comparison to each single agent alone (Fig. 4C and D). The sustained K48-ubiquitin and cPARP accumulation translated into significantly improved antitumor activity (Fig. 4E-F). The combination of CB-5083 and

bortezomib in the AMO-1 model was highly active (TGI 108%– Supplementary Fig. 4D) and when represented in a waterfall plot, the individual data showed an increased response rate with the combination when compared to single agent bortezomib or CB-5083 (Fig. 4E). In RPMI8226 tumors, the combination of suboptimal doses of CB-5083 and carfilzomib showed superiority to both single agents (p=0.0004) (Fig. 4F). In summary, when CB-5083 was combined with PIs, enhanced antitumor effects were observed.

CB-5083 prevents Nrf1 regulation of proteasome transcription

Upon exposure to PIs, mammalian cells increase expression of multiple proteasome subunits which elevate proteasome content and promote survival (22,23). This process is driven by the transcription factor Nrf1/NFE2L1. It was recently demonstrated that p97 is required for this Nrf1-mediated proteasome bounce-back response owing to its activity in retro-translocating Nrf1 from the ER membrane to the cytosol (24). Since this proteasome bounce-back has been described to limit the ability of PIs to kill myeloma cells (25), blocking such a compensatory response through p97 inhibition may provide a mechanism to enhance the efficacy of PIs by co-administration with a p97 inhibitor such as CB-5083. Therefore, we treated RPMI8226 and AMO-1 cells with either CB-5083, bortezomib or the combination of both agents (CB-5083 treatment 1 hr prior to bortezomib) (Fig. 5A). Treatment with bortezomib for 1 hr was not long enough to stabilize Nrf1 (Fig. 5A). At later time points, a low molecular weight band of Nrf1 accumulated in cells treated with bortezomib, whereas after CB-5083 treatment a higher molecular weight band of Nrf1 accumulated. In the combination experiment of both agents, most of the Nrf1 was found as the higher molecular weight band. The low molecular weight

band represents a cleaved and active form of Nrf1 that is translocated to the nucleus where it activates many proteasome subunit genes (PSM; see later Fig. 5C). CB-5083 treatment leads to the accumulation of an uncleaved higher molecular weight form of Nrf1, which corresponds to Nrf1 that is retained in the ER membrane and cannot translocate to the nucleus (Fig. 5C and 5D). The CB-5083 mediated retention of Nrf1 in the ER was observed in additional MM cell lines (Supplementary Fig. S5A) and the dominant CB-5083 phenotype in combination with bortezomib was recapitulated in vivo in RPMI8226 xenografts (Fig. 5B). In A549 cells, CB-5083 prevented the bortezomib induced translocation of Nrf1 to the nucleus in a dose dependent manner (Fig. 5C-D).

Consistent with a block in Nrf1 activation, bortezomib induced expression of proteasome genes PSMA6, PSMC6 and PSMD11 is prevented by co-treatment with CB-5083 (Supplementary Fig. S5B-D). In conclusion, combining CB-5083 with bortezomib prevented the activation of Nrf1 and the downstream activation of proteasome subunit expression.

CB-5083 remains equipotent in models of acquired resistance to PIs

CB-5083 is a protein homeostasis disruptor with a differentiated mechanism of action compared to the PIs and has the potential to be active in multiple myeloma cells resistant to PIs. Therefore CB-5083 was tested against AMO-1 cell line clones that are resistant to bortezomib or carfilzomib (12). AMO1-BtzR has a bortezomib GI_{50} > 100-fold higher than AMO1-WT. A similar shift in sensitivity was seen in the AMO1-CfzR cell line with respect to carfilzomib (Fig. 6B and 6C). Interestingly, each clone possessed significant cross-resistance to

the alternative PI. However, CB-5083 potency was similar in the wild type AMO-1 cells and the AMO1-BtzR and AMO1-CfzR clones (Fig. 6A).

One potential mechanism of resistance to PIs is through interaction of MM cells with the supportive bone marrow stromal compartment (BMSC) (26,27). To assess the influence of BMSCs on CB-5083's anti-myeloma activity, compartment-specific bioluminescence (15) (CS-BLI) assays were performed with MM1.S cells co-cultured in the presence of the BMSC cell lines HS5 and HS27A or primary MM patient-derived BMSC culture, BM-61. In these assays, the MM1.S GI_{50} was 0.53 µM and was unaffected by the presence or absence of BMSCs (Fig. 6D). Furthermore, the GI_{50} against the MM1.S cell compartment was 3-fold and 6-fold lower than the immortalized and primary BMSC compartment GI_{50} alone (1.58 µM for HS5 and 3.18 µM for BM-61). In contrast, carfilzomib demonstrated a marked reduction in potency and decreased anti-myeloma activity in the context of all bone marrow stromal compartments, with its GI_{50} shifting 1.7-2.4-fold, from 21 nM to 36-51 nM in co-culture with BMSCs (Fig. 6E).

Extending the above observations from CS-BLI into patient derived samples, CB-5083 activity was assessed in bone marrow aspirates from MM patients. Twenty-three samples were assessed by flow to measure apoptosis in $CD138^+$ and $CD138^-$ cells, fourteen from newly diagnosed patients and nine from patients that had been previously treated with bortezomib. In the newly diagnosed samples CB-5083 activity varied widely with GI_{50}s ranging from 0.47 to 36.3 µM. However, CB-5083 had GI_{50}s below 1.6 µM in all but one previously treated patient samples (Fig. 6F). In the same bone marrow sample, analysis of CB-5083 activity in $CD138^-$ cells showed lower sensitivity compared to the $CD138^+$ cell population in 16 out of 18 samples

where both types were analyzed (Fig. 6G). These findings suggest that CB-5083 has more cytotoxic activity against MM cells compared to the normal cell population of bone marrow.

In conclusion, CB-5083 was shown to be active against PI adapted cell line models, retained potent anti-myeloma activity in BMSC co-culture models and had potent activity in ex vivo previously treated MM patient samples.

CB-5083 is highly active in mouse models relevant to multiple myeloma

Previously, CB-5083 was shown to be active in a variety of solid tumor models (10). We used an ortho-metastatic mouse model of MM to assess efficacy of CB-5083. Mice were injected IV with MM.1S (Fig. 7A) or RPMI8226 cells (Supplementary Fig. S6A) that were modified to express luciferase. Oral treatment with CB-5083 at a dose of 60 mg/kg on a qd4/3 off schedule inhibited tumor progression to an extent that compared favorably ($p<0.0001$) to IV bortezomib over a three-week dosing cycle (Fig. 7B). CB-5083 demonstrated a similar level of efficacy in the disseminated RPMI8226 tumor model, which again, compared favorably to an effective regimen of IP carfilzomib (Supplementary Fig. S6B).

In a subcutaneous RPMI8226 model, CB-5083 was compared to bortezomib, carfilzomib and ixazomib. In this model, all agents inhibited RPMI8226 growth with CB-5083 showing the highest TGI (Fig. 7C). After three cycles of dosing with CB-5083, tumors were allowed to regrow and were re-challenged with CB-5083 once they reached 700 mm^3 (Supplementary Fig. S6C). CB-5083 was again able to induce 50% regression of these tumors.

Next, CB-5083 activity was investigated in combination with dexamethasone and lenalidomide, two active anti-MM agents (Fig. 7D). Suboptimal doses of CB-5083 combined with suboptimal doses of dexamethasone and lenalidomide led to regression of tumors, demonstrating the superiority of the triple combination arm ($p<0.0001$). These findings were consistent with the level of lambda light chains quantified in the plasma of the tumor bearing mice (Supplementary Fig. S6D).

Finally, CB-5083 antitumor activity was evaluated in the Vk*MYC model, a transgenic mouse model that reproduces the pathogenesis, biology, and clinical features of MM and is predictive of clinical activity (18,28). Prior to dosing, baseline serum M-spike was determined by serum protein electrophoresis (SPEP) in individual mice. CB-5083 was administered orally for 2 weekly cycles in C57/BL6 Vk*MYC mice. On Day 14, SPEP analysis of serum showed a 55% decrease in M-spike when compared to pre-dose levels (Fig. 7E). Taken together, CB-5083 showed potent antitumor activity in a wide variety of clinically relevant in vivo MM models.

Discussion

It has been well documented that myeloma cells are exquisitely sensitive to perturbation of protein homeostasis, owing to their high rates of immunoglobulin synthesis and secretion (4). Pharmacological inhibition of the chymotryptic site of the proteasome exhibits potent clinical activity in myeloma, Waldenström's macroglobulinemia and amyloidosis (1,29,30). These observations suggest that the activity of proteasome inhibition in MM may represent an effect against the intrinsic biology of plasma cells rather than the specific oncogenic events harbored by the MM cells.

The current study examines the phenotypic consequences of pharmacological inhibition of p97/VCP using CB-5083 in pre-clinical models of MM. p97 plays important roles in protein homeostasis upstream of the proteasome and CB-5083 has recently been described as a novel anti-cancer agent targeting p97. CB-5083 appears to be quite selective for the ERAD-related functions of p97, with only minor (if any) effects on its other cellular functions. This relative selectivity of CB-5083 for the ERAD-related functions of p97 renders it an attractive option for the treatment of MM, which exhibits pronounced responsiveness upon pharmacological perturbation of ERAD. As p97 was demonstrated to be involved in the regulation of other oncogenic pathways (including NFκB (31) or HIF1α (32)), further study of the non-ER functions of p97 that may be affected by CB-5083 and may have been missed by the gene ontology analysis are warranted.

Based on these considerations, we set out to characterize the response to CB-5083 in models of multiple myeloma. We observed that submicromolar concentrations of CB-5083 were capable of inducing a significant decrease in viability for the majority of MM cell lines tested. The observed GI_{50} values for MM cell lines were significantly lower than those observed for non-MM cell lines tested in this work or previously (10). The exquisite sensitivity of MM cells to CB-5083 could be explained by a much higher level of ER stress and UPR at baseline, in comparison to solid tumor cell lines. In viability assays, there was little correlation between the sensitivity of MM cell lines to CB-5083 and their sensitivity to PIs. The anti-MM activity of CB-5083 was not significantly attenuated by in vitro interactions of MM cells with BMSCs. This can be viewed as

a favorable phenotypic result, given BMSCs confer resistance to anti-MM agents via cell adhesion–mediated drug resistance (15,26). The preclinical anti-MM activity of CB-5083 was associated with potent induction of canonical markers of the UPR, including phosphorylation of PERK, accumulation of sXBP1 and BiP, and induction of CHOP, as well as accumulation of K48-linked poly-ubiquitin, a hallmark of inhibition of protein degradation. Despite some of the similarities in gene expression changes seen in response to CB-5083 and PIs, CB-5083 did exhibit some distinct features. The transcriptional profile of CB-5083-treated MM cells lacked the pronounced upregulation of heat shock genes or proteasome subunits, which has been reported to reflect compensatory responses mounted by MM cells in the context of 20S proteasome inhibition (22,33). These distinct events for CB-5083 vs PIs may be related to the differential impact of these classes of drugs on post-translational processing, intracellular localization and transcriptional activity of Nrf1. Unlike bortezomib or carfilzomib, CB-5083 treatment is associated with inhibition of Nrf1 cleavage and its retention in the ER membrane, thereby preventing its nuclear translocation and transcription of proteasome subunit genes. Notably, Nrf1-mediated induction of proteasome gene expression is thought to limit the cytotoxic effects of the UPR in myeloma cells in response to PIs (24,25,34,35).

CB-5083 enhanced the anti-MM activity of bortezomib both in vitro and in vivo and was active in bortezomib resistance models as well as primary MM cells derived from patients who had been treated with bortezomib-based regimens. The observation that CB-5083 decreases the myeloma tumor burden in the Vk*MYC genetically engineered mouse model of myeloma is also notable, because it suggests that p97 inhibition may have utility at different stages of the disease. This model is considered to capture the behavior of MM in its earlier stages whereas xenografts of human myeloma cell lines are considered to be reflective of the molecular features of advanced MM (18,28).

An important area of investigation relates to the characterization of molecular markers that may identify myeloma cells with pronounced responses to CB-5083 monotherapy. Indeed, some of the myeloma cell lines tested in our studies exhibited more potent and/or rapid

responses to CB-5083 compared to other cell lines in the panel. Our current study was not designed to identify such candidate markers, but it is reasonable to hypothesize that these markers may prove to be quite distinct from those associated with potent responses to PIs given that the quantitative patterns of response of MM cells to these agents differ substantially from the observed pattern for CB-5083. In a separate recent study from our group on the impact of CB-5083 on a large panel of solid tumor cell lines, mutational activation of Ras/Raf/MAPK signaling exhibited a trend for a higher degree of responsiveness to CB-5083 (10). MM also exhibits frequent activation of Ras/Raf/MAPK signaling through mutations in diverse components of this pathway (36) and/or cell non-autonomous activation in the context of tumor microenvironment interactions (26,37). We were able to demonstrate on a smaller panel of MM cells listed in Anderson et al paper (AMO-1, RPMI8226, OPM2, MM1-S and MM1-R) that there was a strong correlation between MM tumor responses and phospho/total ERK ratio (unpublished analysis (10)). We envision that validation of this hypothesis in studies of larger cell line panels or in samples from patients in clinical trials of CB-5083 may represent a path toward confirming or refuting whether CB-5083 might play an important role in the treatment of MM patients with mutations in the Ras/Raf/MAPK pathway.

In summary, CB-5083 has demonstrated robust pre-clinical activity via a novel and distinctive mechanism of action. Currently clinical trials are ongoing in patients with multiple myeloma who have exhausted other available therapies.

Acknowledgments

We thank Drs. Suzanne Trudel, Joan Levy, Jesse Vargas and Daniel Auclair for scientific discussion and contributions to work presented in this manuscript.

This work was funded in part by the Multiple Myeloma Research Foundation (B.T.A), The Myeloma Fund of the Silicon Valley Community Foundation (B.T.A.), and The Stephen and Nancy Grand Multiple Myeloma Translational Initiative (B.T.A.). C.D. was supported by a grant from Oncosuisse.

Correspondence: Ronan Le Moigne, Cleave Biosciences, 866 Malcolm Rd, #100, Burlingame. CA, 94010, E-mail : ronan.lemoigne29@gmail.com

References

1. Richardson PG, Barlogie B, Berenson J, Singhal S, Jagannath S, Irwin D*, et al.* A phase 2 study of bortezomib in relapsed, refractory myeloma. N Engl J Med **2003**;348:2609-17
2. Fisher RI, Bernstein SH, Kahl BS, Djulbegovic B, Robertson MJ, de Vos S*, et al.* Multicenter phase II study of bortezomib in patients with relapsed or refractory mantle cell lymphoma. J Clin Oncol **2006**;24:4867-74
3. Teicher BA, Anderson KC. CCR 20th anniversary commentary: In the beginning, there was PS-341. Clin Cancer Res **2015**;21:939-41
4. Boise LH, Kaufman JL, Bahlis NJ, Lonial S, Lee KP. The Tao of myeloma. Blood **2014**;124:1873-9
5. Magnaghi P, D'Alessio R, Valsasina B, Avanzi N, Rizzi S, Asa D*, et al.* Covalent and allosteric inhibitors of the ATPase VCP/p97 induce cancer cell death. Nat Chem Biol **2013**;9:548-56
6. Deshaies RJ. Proteotoxic crisis, the ubiquitin-proteasome system, and cancer therapy. BMC Biol **2014**;12:94
7. Buchberger A, Schindelin H, Hanzelmann P. Control of p97 function by cofactor binding. FEBS Lett **2015**;589:2578-89
8. Wojcik C, Yano M, DeMartino GN. RNA interference of valosin-containing protein (VCP/p97) reveals multiple cellular roles linked to ubiquitin/proteasome-dependent proteolysis. J Cell Sci **2004**;117:281-92
9. Wojcik C, Rowicka M, Kudlicki A, Nowis D, McConnell E, Kujawa M*, et al.* Valosin-containing protein (p97) is a regulator of endoplasmic reticulum stress and of the degradation of N-end rule and ubiquitin-fusion degradation pathway substrates in mammalian cells. Mol Biol Cell **2006**;17:4606-18
10. Anderson DJ, Le Moigne R, Djakovic S, Kumar B, Rice J, Wong S*, et al.* Targeting the AAA ATPase p97 as an Approach to Treat Cancer through Disruption of Protein Homeostasis. Cancer Cell **2015**;28:653-65
11. Zhou HJ, Wang J, Yao B, Wong S, Djakovic S, Kumar B*, et al.* Discovery of a First-in-Class, Potent, Selective and Orally Bioavailable Inhibitor of the p97 AAA ATPase (CB-5083). J Med Chem **2015**
12. Ruckrich T, Kraus M, Gogel J, Beck A, Ovaa H, Verdoes M*, et al.* Characterization of the ubiquitin-proteasome system in bortezomib-adapted cells. Leukemia **2009**;23:1098-105
13. Soriano GP, Besse L, Li N, Kraus M, Besse A, Meeuwenoord N*, et al.* Proteasome inhibitor-adapted myeloma cells are largely independent from proteasome activity and show complex proteomic changes, in particular in redox and energy metabolism. Leukemia **2016**
14. Bennett TA, Montesinos P, Moscardo F, Martinez-Cuadron D, Martinez J, Sierra J*, et al.* Pharmacological profiles of acute myeloid leukemia treatments in patient samples by automated flow cytometry: a bridge to individualized medicine. Clin Lymphoma Myeloma Leuk **2014**;14:305-18
15. McMillin DW, Delmore J, Weisberg E, Negri JM, Geer DC, Klippel S*, et al.* Tumor cell-specific bioluminescence platform to identify stroma-induced changes to anticancer drug activity. Nat Med **2010**;16:483-9
16. McMillin DW, Jacobs HM, Delmore JE, Buon L, Hunter ZR, Monrose V*, et al.* Molecular and cellular effects of NEDD8-activating enzyme inhibition in myeloma. Mol Cancer Ther **2012**;11:942-51
17. Edgar R, Domrachev M, Lash AE. Gene Expression Omnibus: NCBI gene expression and hybridization array data repository. Nucleic Acids Res **2002**;30:207-10

18. Chesi M, Matthews GM, Garbitt VM, Palmer SE, Shortt J, Lefebure M*, et al.* Drug response in a genetically engineered mouse model of multiple myeloma is predictive of clinical efficacy. Blood **2012**;120:376-85
19. Chou TF, Brown SJ, Minond D, Nordin BE, Li K, Jones AC*, et al.* Reversible inhibitor of p97, DBeQ, impairs both ubiquitin-dependent and autophagic protein clearance pathways. Proc Natl Acad Sci U S A **2011**;108:4834-9
20. D'Arcy P, Brnjic S, Olofsson MH, Fryknas M, Lindsten K, De Cesare M*, et al.* Inhibition of proteasome deubiquitinating activity as a new cancer therapy. Nat Med **2011**;17:1636-40
21. Kuhn DJ, Chen Q, Voorhees PM, Strader JS, Shenk KD, Sun CM*, et al.* Potent activity of carfilzomib, a novel, irreversible inhibitor of the ubiquitin-proteasome pathway, against preclinical models of multiple myeloma. Blood **2007**;110:3281-90
22. Mitsiades N, Mitsiades CS, Poulaki V, Chauhan D, Fanourakis G, Gu X*, et al.* Molecular sequelae of proteasome inhibition in human multiple myeloma cells. Proc Natl Acad Sci U S A **2002**;99:14374-9
23. Sha Z, Goldberg AL. Proteasome-mediated processing of Nrf1 is essential for coordinate induction of all proteasome subunits and p97. Curr Biol **2014**;24:1573-83
24. Radhakrishnan SK, den Besten W, Deshaies RJ. p97-dependent retrotranslocation and proteolytic processing govern formation of active Nrf1 upon proteasome inhibition. Elife **2014**;3:e01856
25. Radhakrishnan SK, Lee CS, Young P, Beskow A, Chan JY, Deshaies RJ. Transcription factor Nrf1 mediates the proteasome recovery pathway after proteasome inhibition in mammalian cells. Mol Cell **2010**;38:17-28
26. Markovina S, Callander NS, O'Connor SL, Xu G, Shi Y, Leith CP*, et al.* Bone marrow stromal cells from multiple myeloma patients uniquely induce bortezomib resistant NF-kappaB activity in myeloma cells. Mol Cancer **2010**;9:176
27. Hideshima T, Mitsiades C, Tonon G, Richardson PG, Anderson KC. Understanding multiple myeloma pathogenesis in the bone marrow to identify new therapeutic targets. Nat Rev Cancer **2007**;7:585-98
28. Chesi M, Robbiani DF, Sebag M, Chng WJ, Affer M, Tiedemann R*, et al.* AID-dependent activation of a MYC transgene induces multiple myeloma in a conditional mouse model of post-germinal center malignancies. Cancer Cell **2008**;13:167-80
29. Treon SP, Hunter ZR, Matous J, Joyce RM, Mannion B, Advani R*, et al.* Multicenter clinical trial of bortezomib in relapsed/refractory Waldenstrom's macroglobulinemia: results of WMCTG Trial 03-248. Clin Cancer Res **2007**;13:3320-5
30. Reece DE, Hegenbart U, Sanchorawala V, Merlini G, Palladini G, Blade J*, et al.* Efficacy and safety of once-weekly and twice-weekly bortezomib in patients with relapsed systemic AL amyloidosis: results of a phase 1/2 study. Blood **2011**;118:865-73
31. Asai T, Tomita Y, Nakatsuka S, Hoshida Y, Myoui A, Yoshikawa H*, et al.* VCP (p97) regulates NFkappaB signaling pathway, which is important for metastasis of osteosarcoma cell line. Jpn J Cancer Res **2002**;93:296-304
32. Alexandru G, Graumann J, Smith GT, Kolawa NJ, Fang R, Deshaies RJ. UBXD7 binds multiple ubiquitin ligases and implicates p97 in HIF1alpha turnover. Cell **2008**;134:804-16
33. Shringarpure R, Catley L, Bhole D, Burger R, Podar K, Tai YT*, et al.* Gene expression analysis of B-lymphoma cells resistant and sensitive to bortezomib. Br J Haematol **2006**;134:145-56
34. Meiners S, Heyken D, Weller A, Ludwig A, Stangl K, Kloetzel PM*, et al.* Inhibition of proteasome activity induces concerted expression of proteasome genes and de novo formation of Mammalian proteasomes. J Biol Chem **2003**;278:21517-25

35. Steffen J, Seeger M, Koch A, Kruger E. Proteasomal degradation is transcriptionally controlled by TCF11 via an ERAD-dependent feedback loop. Mol Cell **2010**;40:147-58
36. Kortuem KM, Braggio E, Bruins L, Barrio S, Shi CS, Zhu YX*, et al.* Panel sequencing for clinically oriented variant screening and copy number detection in 142 untreated multiple myeloma patients. Blood Cancer J **2016**;6:e397
37. Murray ME, Gavile CM, Nair JR, Koorella C, Carlson LM, Buac D*, et al.* CD28-mediated pro-survival signaling induces chemotherapeutic resistance in multiple myeloma. Blood **2014**;123:3770-9

Figure legends

Figure 1.

Effect of CB-5083 on cell growth and survival in MM and solid tumor cell lines. A, multiple myeloma cell lines expressing FF-Luc were treated with a dose titration of CB-5083 for 72 hr, followed by measurement of viability using BLI. B, a panel of solid tumor cell lines (n=153) and MM cell lines (n = 7), were treated with CB-5083 for 24, 40 and 72 hr, and cell viability (box plot ± min and max) was determined using the Cell Titer Glow assay. C, genes overexpressed in MM with a p-value <0.001 were analyzed using ENRICHR. Mean gene expression values were calculated for all solid tumor derived cell lines versus MM cell lines using the CCLE gene expression data. Difference in gene expression between the two cell groups was calculated using a student's t-test. D, time course evaluation of viability of cell lines treated with 2.5 µM CB-5083 for various amounts of time with cell death read-out at 72 hr using the Cell Titer Glow assay. E, time course evaluation of caspase 3/7 induction in cell lines treated with 2.5 µM CB-5083 by Caspase 3/7-Glo assay. All data representative of ≥ 2 experiments.

Figure 2.

CB-5083 activates UPR and apoptosis of MM cell lines in vitro and in vivo. A, RPMI8226 cells were treated with dimethylsulfoxide (DMSO), CB-5083 (0.3125-20 µM), bortezomib (6.25–400 nM) or thapsigargin (12.5-800 nM) during 8 hr. Protein lysates were subjected to immunoblotting with anti-BiP, XBP1s, PERK, CHOP, K48 ubiquitin or GAPDH antibodies. B, SCID Beige mice bearing RPMI8226 tumors (n=3-4/group) were received a single p.o. dose of CB-5083 at 60 mg/kg. Tumors were collected at 1, 6 and 24 hr post dose and tumor lysates were

subjected to MSD analysis for K48 Ubiquitin. Plasma from the same mice was collected and levels of CB-5083 were determined by LC-MS and plotted with K48-Ub modulation. C, the same tumor lysates were subjected to measurement of CHOP and cPARP protein levels by MSD.

Figure 3.

CB-5083 activity is different than PIs. A-C, the viability GI_{50} for the 18 MM cell line panel were generated for carfilzomib (A), bortezomib (B) and CB-5083 (C), then plotted and compared for each pair of agents. D, transcriptomic data were generated in RPMI8226, MM1.S and AMO-1 cells treated for 6 hr with a high (1 μM for RPMI8226 & MM1S; 500 nM for AMO-1) or a low (500 nM for RPMI8226 & MM1S; 100 nM for AMO-1) dose of CB-5083, or bortezomib (10 nM). Gene expression heat maps were generated using GENE-E software. E-F, gene ontology analysis was performed on gene lists obtained after RNAseq analysis, sorted by magnitude of differential expression after bortezomib or CB-5083 treatment in RPMI8226 (E) or AMO-1 (F) cells, by GO biological processes enrichment analysis using Enrichr.

Figure 4.

Combination of CB-5083 with bortezomib showed enhanced cytotoxic effect in MM. A-B, viability of RPMI8226 cells over a range of CB-5083 doses as a single agent (black) and in the presence of varying doses of bortezomib (A) or carfilzomib (B) (colored). Percentage viability was determined by normalizing to viability obtained in the DMSO control group. Cells were treated continuously with CB-5083 and PIs for 72 hr and then assessed for viability by using Cell

Titer Glow Assay. C-D, PD evaluation in SCID Beige mice bearing RPMI8226 tumors (n=3-4/group). Mice were received a single p.o. dose of CB-5083 at 60 mg/kg, bortezomib at 0.8 mg/kg or the combination of both agents. Tumors were collected at 1, 6 and 24 hr post dose and tumor lysates were subjected to MSD analysis for K48-Ub (C) or cPARP (D). E, waterfall plot representation of tumor response at individual mouse level in AMO-1 xenografts treated with CB-5083, bortezomib or both agents in combination (n=8-9/group). For each animal, the best average response was calculated as the minimal value of tumor volume change at time *t* to its baseline, with *t*>10 days. CB-5083 was dosed qd4/3off, p.o. at 50 mg/kg, and bortezomib biw, i.v. at 0.8 mg/kg. Traditional growth curve of the same experiment is represented in supplementary Fig. S4. F, RPMI8226 cells (10 millions) were subcutaneously inoculated into SCID Beige mouse hind flank region. When the tumors reached 200-300 mm^3, mice were randomized in treatment groups (9 mice in each group) and treated with CB-5083 and carfilzomib vehicles, CB-5083 (30 mg/kg – qd4/3off), carfilzomib (3 mg/kg, qd2/5off) or combination of both agents for 18 days. All data representative of ≥ 2 experiments.

Figure 5.

The Nrf1 upregulation induced by bortezomib is inhibited by CB-5083. A, AMO-1 and RPMI8226 MM1.S cells were treated with either bortezomib (10 nM), CB-5083 (1 μM) or in combination, with CB-5083 administered 1hr prior to bortezomib. Protein lysate were immunoblotted at different time points with anti- Nrf1 and GAPDH antibodies. B, SCID Beige mice, bearing RPMI8226 tumors (n=3-4/group) received a single p.o. dose of CB-5083 at 60 mg/kg, and 1 hour later a single dose of bortezomib at 0.8 mg/kg or the combination of both agents. Tumor were

collected at 2, 6 and 24 hr post CB-5083 dose and tumor lysates were subjected to immunoblot of Nrf1. C, immunofluorescence of Nrf1 and nucleus in A549 adherent cells. Cells were treated with 1 µM of bortezomib, 10 µM of CB-5083, or with the combination of both agents for 8 hr. D, The levels of Nrf1 in the nucleus were measured.

Figure 6.

CB-5083 activity in models of proteasome adaptation. A-C, CB-5083 (A), bortezomib (B) or carfilzomib (C) were tested in AMO-1 WT, bortezomib resistant and –carfilzomib resistant cell lines, treated 72 hr with each agent. D-E, MM.1S cells were cultured alone or with BMSCs in the presence or either CB-5083 (D) or carfilzomib (E), and viability was measured by compartment-specific bioluminescence (CS-BLI) assays. F, 14 chemotherapy naïve and 9 refractory or resistant primary multiple myeloma specimen were treated with a dose titration of CB-5083 for 24 hr, and their viability was measured by flow cytometry. A-F data representative of multiple experiments. G, primary multiple myeloma samples ($CD38^-/138+$) and their matching normal population ($CD38^-/138^-$) were treated with CB-5083 for 24 hr. The EC50 of each patient sample was then matched between the $CD38^+/138^+$ and $CD38^-/138^-$ population.

Figure 7.

CB-5083 demonstrates a broad activity in in vivo relevant MM models. A-B, $1x10^6$ MM1.S–Luc cells were injected by the tail vein in NSG mice. On day 12, mice were randomized (n=5/group) in a vehicle group, CB-5083 (60 mg/kg, qd4/3off) and bortezomib (1 mg/kg, biw).

Bioluminescence signal was captured on day 12 and 25 of treatment, and the flux signal was quantified in graph (B). C, SCID Beige mice bearing established RPMI8226 tumors (n=10/group) were treated with vehicle (0.5% methyl cellulose), CB-5083 (100 mg/kg, p.o., qd4/3off), bortezomib (1 mg/kg, i.v., biw), carfilzomib (5 mg/kg, i.v.,qd2/5off) or ixazomib (11 mg/kg, p.o., biw) during 18 days. D, SCID Beige mice bearing advanced (> 300 mm^3) RPMI8226 tumors (n=10/group), were treated with vehicle, CB-5083 (40 mg/kg, p.o., qd4/3off), a combination of dexamethasone (0.1 mg/kg, i.p., qd) + lenalidomide (20 mg/kg, p.o., qd) or the triple combination CB-5083 / dexamethasone / lenalidomide, during 25 days. E, three Vk*MYC mice were treated with CB-5083 (30 mg/kg, p.o. qd4/3off) during 14 days. M-protein was measured by SPEP predose day 0 and day 14 post treatment.

Author Manuscript Published OnlineFirst on September 6, 2017; DOI: 10.1158/1535-7163.MCT-17-0233
Author manuscripts have been peer reviewed and accepted for publication but have not yet been edited.

Figure 1

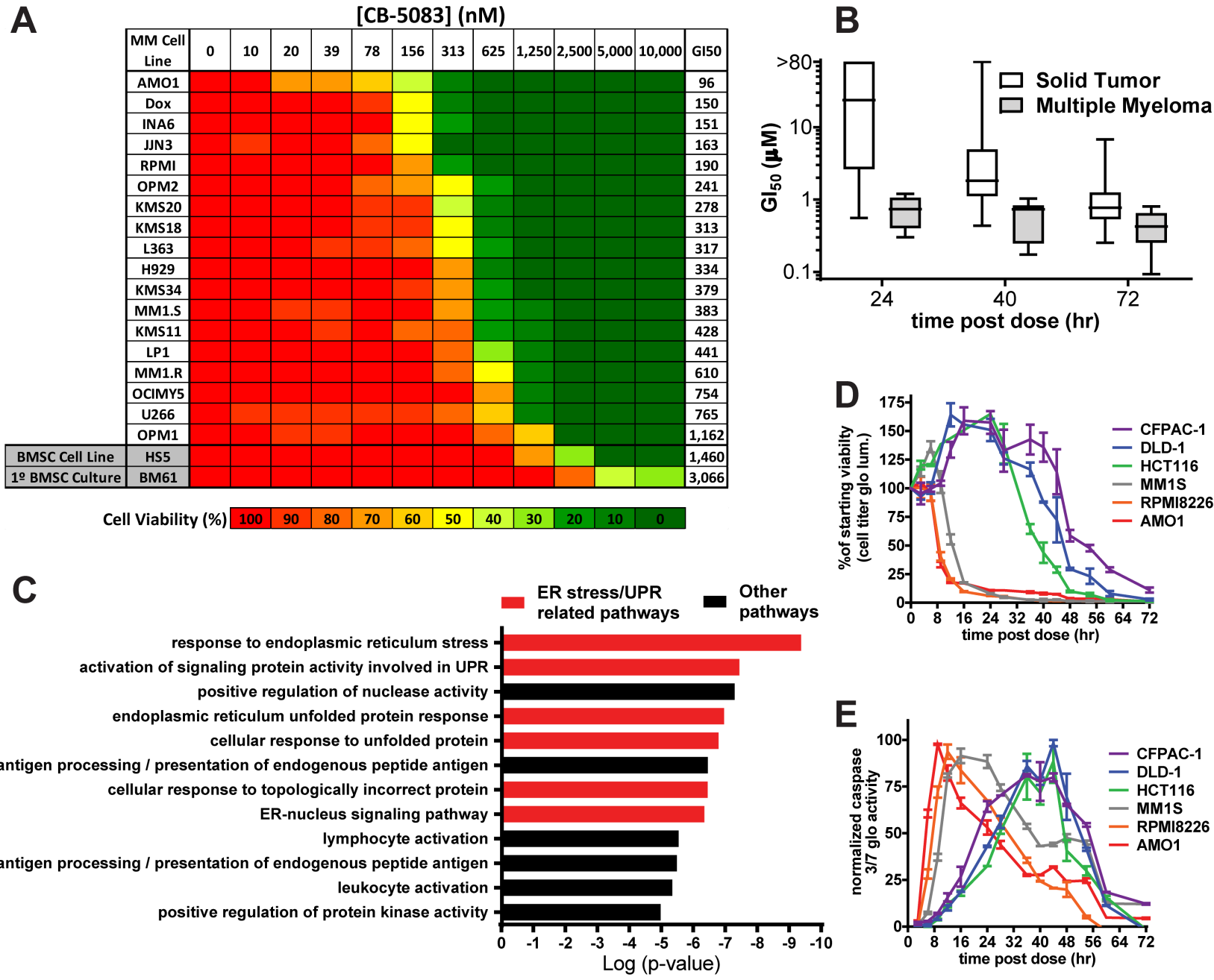

Author Manuscript Published OnlineFirst on September 6, 2017; DOI: 10.1158/1535-7163.MCT-17-0233
Author manuscripts have been peer reviewed and accepted for publication but have not yet been edited.

Figure 2

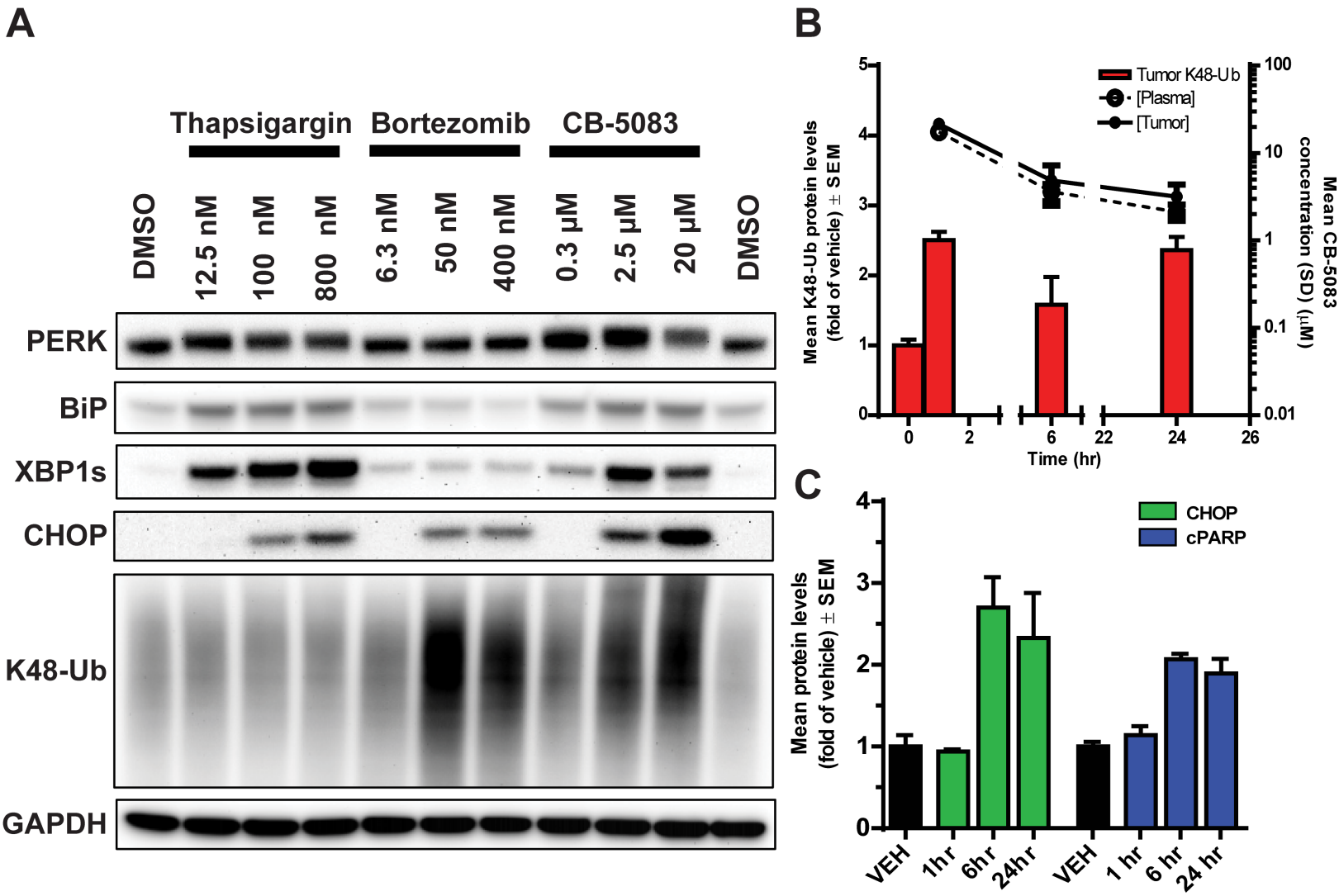

Author Manuscript Published OnlineFirst on September 6, 2017; DOI: 10.1158/1535-7163.MCT-17-0233
Author manuscripts have been peer reviewed and accepted for publication but have not yet been edited.

Figure 3

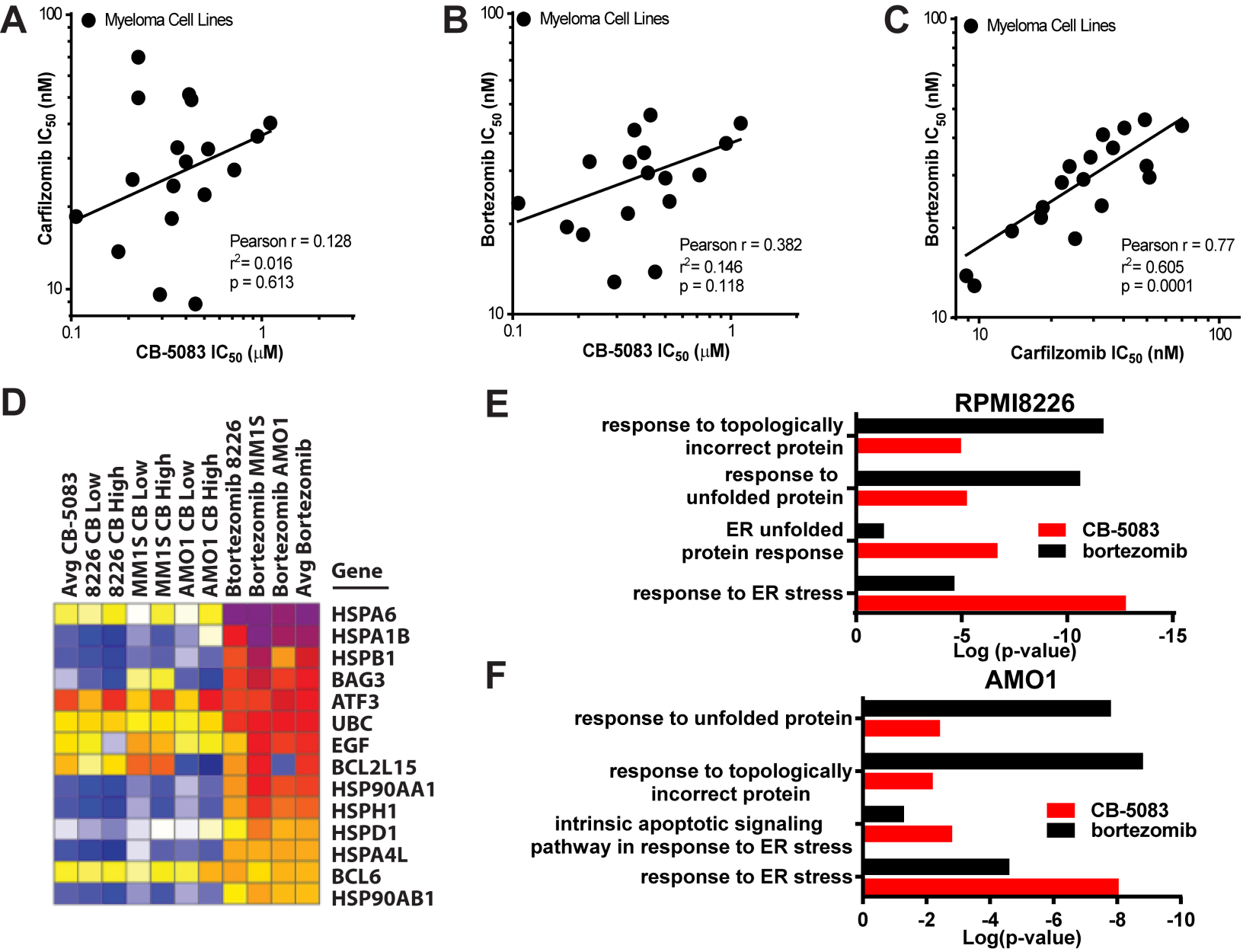

Author Manuscript Published OnlineFirst on September 6, 2017; DOI: 10.1158/1535-7163.MCT-17-0233
Author manuscripts have been peer reviewed and accepted for publication but have not yet been edited.

Figure 4

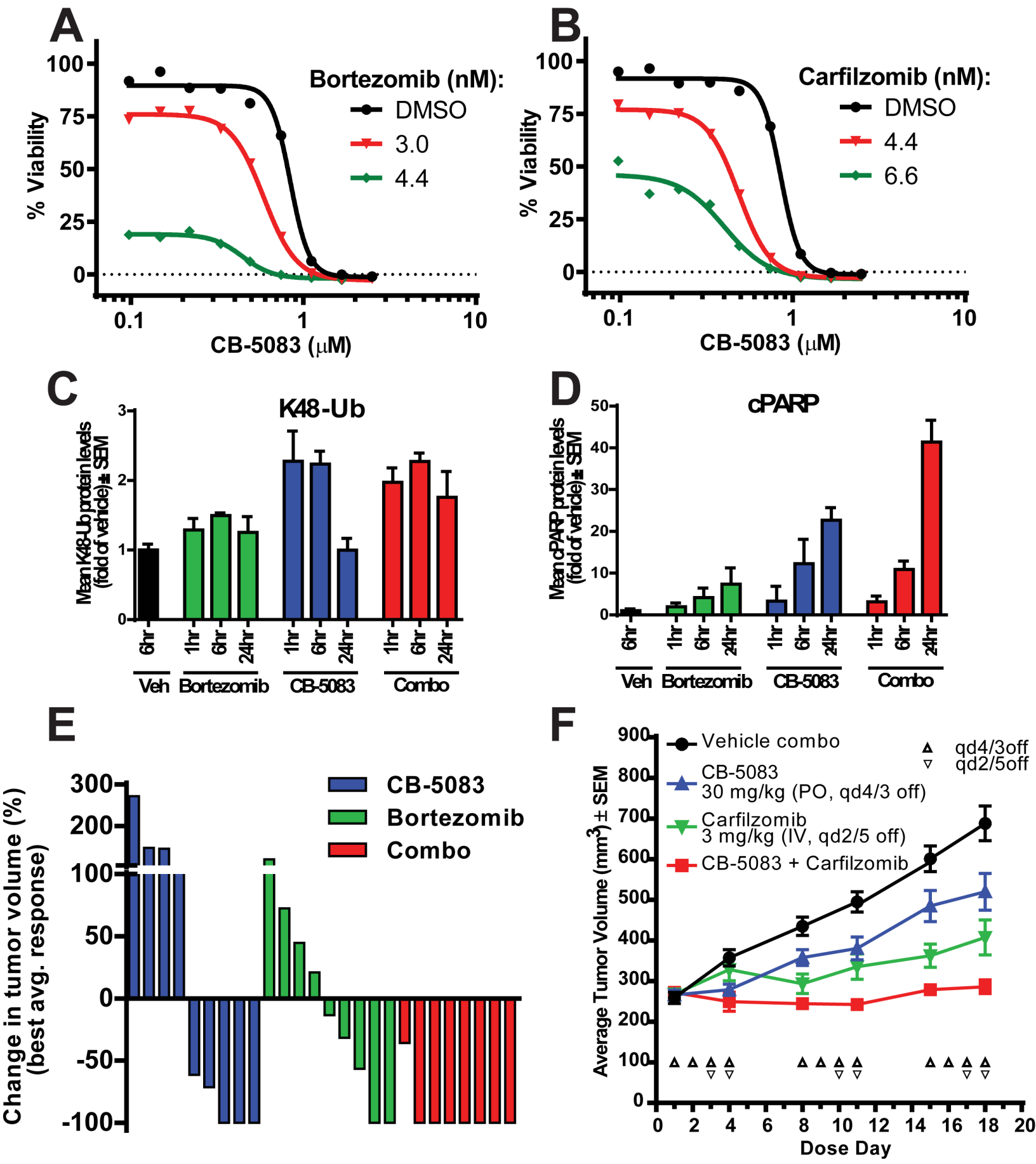

Author Manuscript Published OnlineFirst on September 6, 2017; DOI: 10.1158/1535-7163.MCT-17-0233
Author manuscripts have been peer reviewed and accepted for publication but have not yet been edited.

Figure 5

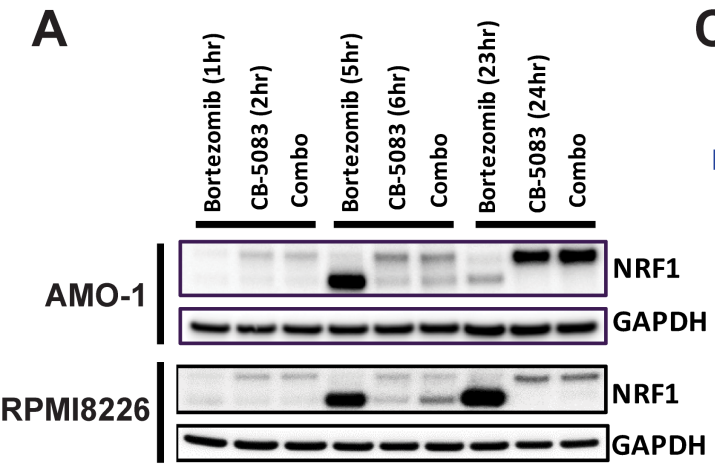

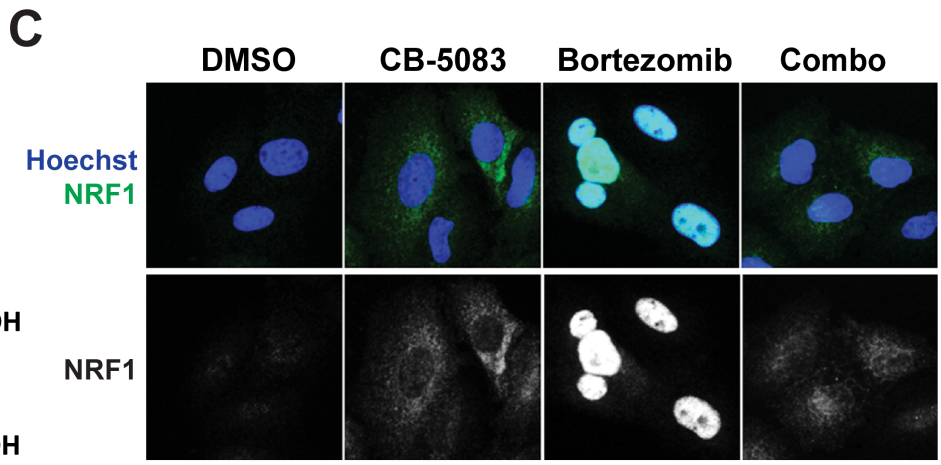

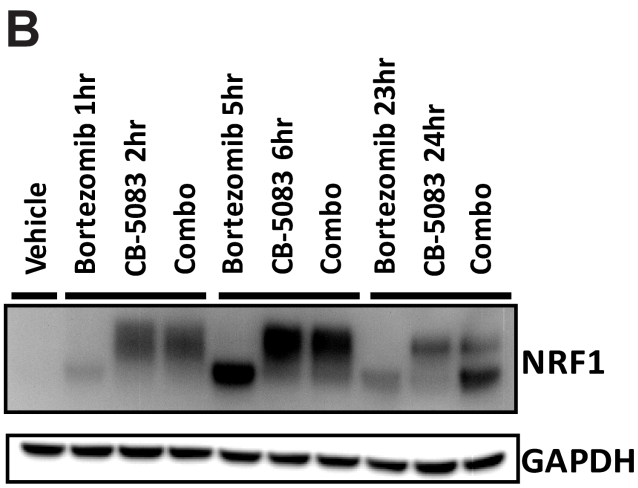

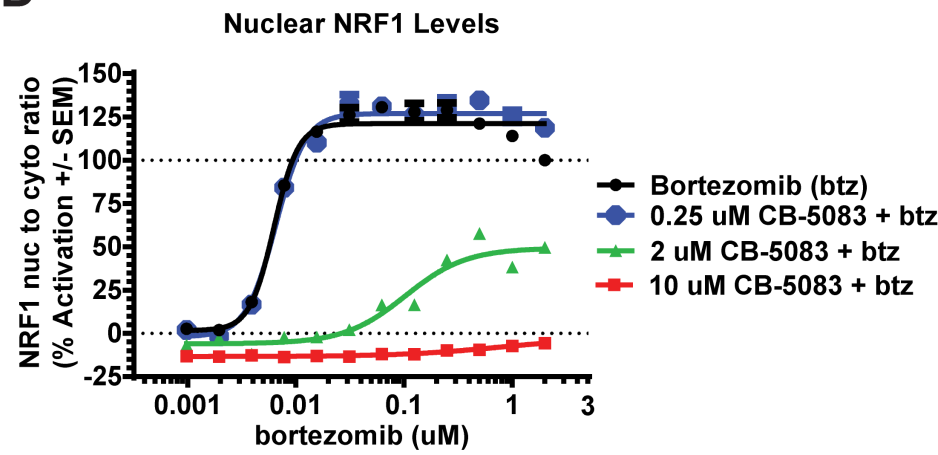

Author Manuscript Published OnlineFirst on September 6, 2017; DOI: 10.1158/1535-7163.MCT-17-0233
Author manuscripts have been peer reviewed and accepted for publication but have not yet been edited.

Figure 6

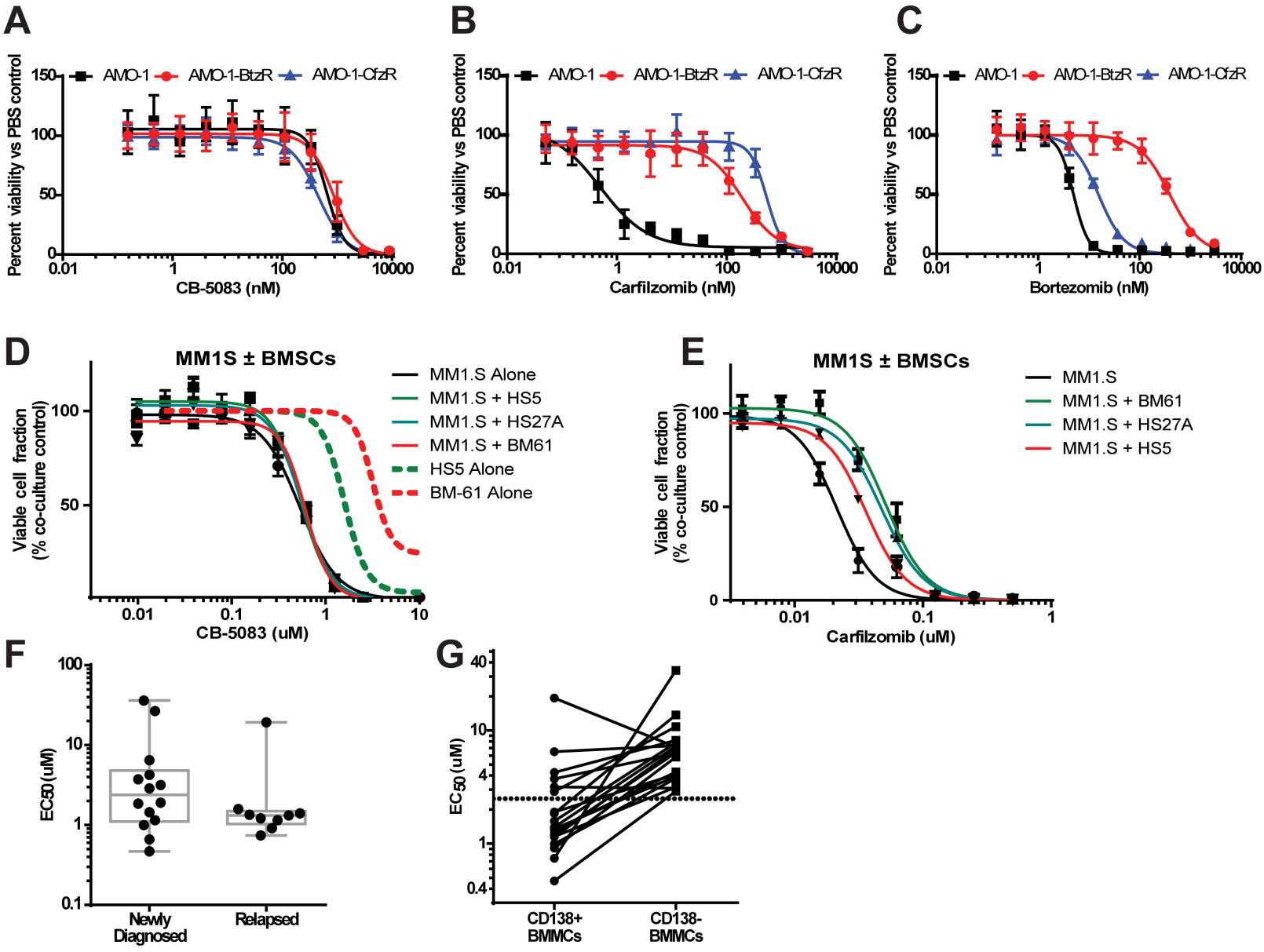

Author Manuscript Published OnlineFirst on September 6, 2017; DOI: 10.1158/1535-7163.MCT-17-0233
Author manuscripts have been peer reviewed and accepted for publication but have not yet been edited.

Figure 7

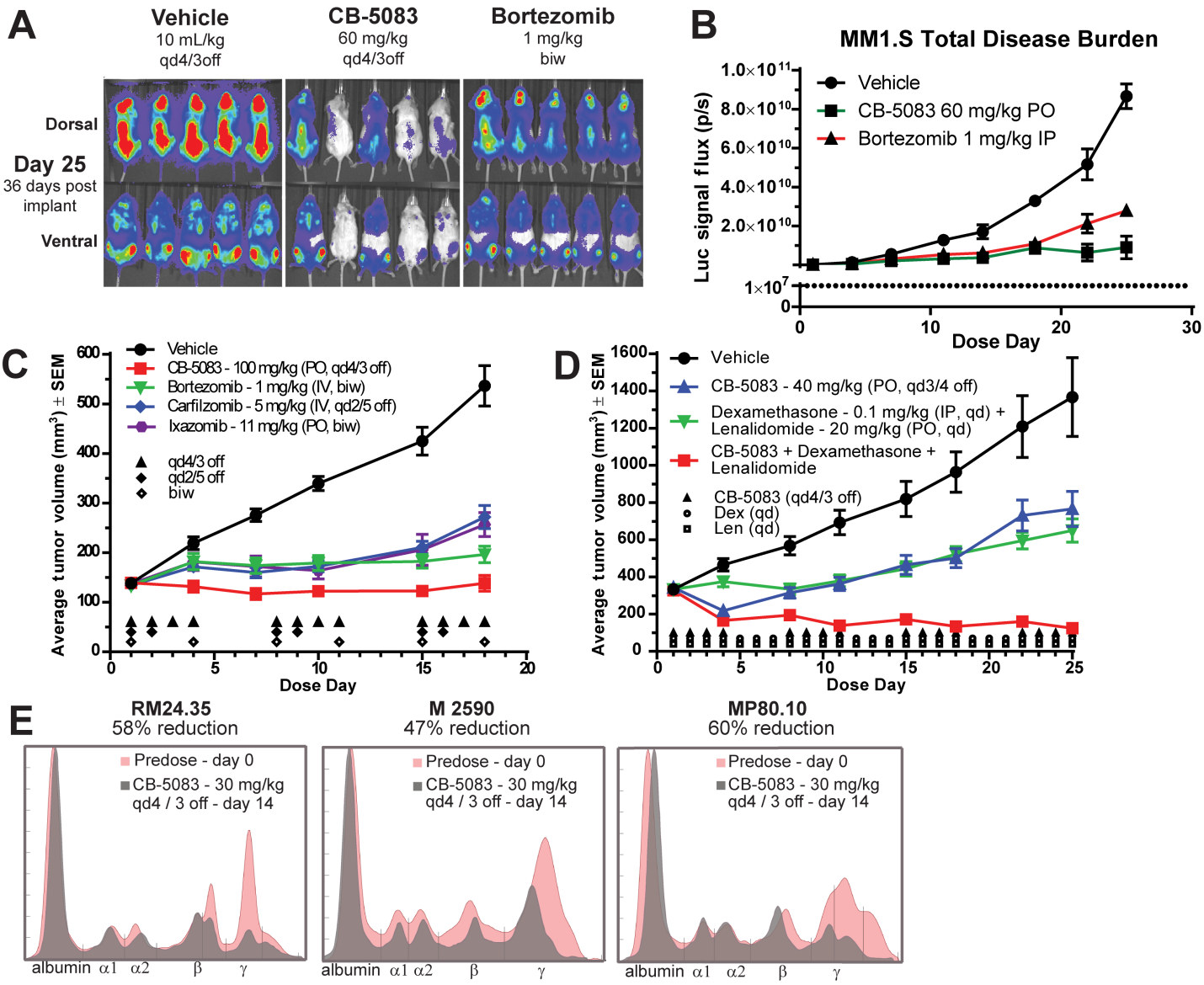

AACR American Association for Cancer Research

Molecular Cancer Therapeutics

The p97 inhibitor CB-5083 is a unique disrupter of protein homeostasis in models of Multiple Myeloma.

Ronan Le Moigne, Blake T. Aftab, Stevan Djakovic, et al.

Mol Cancer Ther Published OnlineFirst September 6, 2017.